Additional multi-proxy stalagmite evidence from northeast Namibia supports recent models of wetter conditions during the 4.2 ka Event in the Southern Hemisphere

L. Bruce Railsback[a,*], Fuyuan Liang[b], George A. Brook[c], Hai Cheng[d,e], R. Lawrence Edwards[e]

[a] *Department of Geology, University of Georgia, Athens, GA 30602, USA*
[b] *Department of Geography, Western Illinois University, 1 University Circle, Macomb, IL 61455, USA*
[c] *Department of Geography, University of Georgia, Athens, GA 30602, USA*
[d] *College of Global Environmental Change, Xi'an Jiaotong University, Xi'an, Shaanxi 710049, China*
[e] *Department of Earth Sciences, University of Minnesota, Minneapolis, MN 55455, USA*

[*] Corresponding author at: Department of Geology, University of Georgia, Athens, GA 30602, USA.
E-mail address: rlsbk@gly.uga.edu (L.B. Railsback).

Abstract

The 4.2 ka Event has generally been regarded as a period of decades to at most a few centuries in which comparatively dry conditions existed in the Middle East and more broadly across the mid-latitude Northern Hemisphere. This paper presents new stable-isotopic and petrographic observations from two previously-unreported U-Th-dated stalagmites from Dante Cave in northeastern Namibia. The results are most compatible with wetter conditions during the 4.2 ka Event, and wetness during the 4.2 ka Event is the only inference supported by evidence. These new results add to observations previously reported from a third Dante Cave stalagmite suggesting a comparatively wet 4.2 ka Event in which Africa's Tropical Rain Belt migrated southward and rainfall increased along the Congo Air Boundary and/or Kalahari Discontinuity. The new results support findings from three other locations in Namibia and Botswana, from at least seven other locations in the Southern Hemisphere, and at least one in southern China, that suggest a wetter rather than drier 4.2 ka Event in those regions. The pattern emerging from these sites generally agrees with recent modeling results indicating increased moisture over broad areas (but not all) of the Southern Hemisphere. This in turn suggests a 4.2 ka Event that was not a global drought but was instead a set of latitudinally-dependent responses to global-scale southward migration of the Inter-Tropical Convergence Zone (ITCZ), and thus Africa's loosely linked Tropical Rain Belt, as a result of cooling of the Northern Hemisphere, which brought drier conditions to some areas and wetter conditions to others.

Keywords

Holocene, paleoclimate, southern Africa, rainfall, Dante Cave, climate change

1. Introduction: The variability of the 4.2 ka Event

The 4.2 ka Event has been widely investigated both as a significant climatic event and as a driver of societal change (Weiss et al., 1993; Ran and Chen, 2019; Bini et al., 2019). The event was recognized initially in the mid-latitude regions of southwestern Asia (Weiss et al., 1993: Lemcke and Sturm, 1997; Bar-Matthews et al., 1999) but more recently as far north as Iceland (Geirsdóttir et al., 2019) and as far south as southern Patagonia (Ohlendorf et al., 2014).

This widespread recognition of the 4.2 ka Event in part hinges on a willingness to accept phenomena that were seemingly not coeval and that were not of the same nature. With regard to the timing of the event, Railsback et al. (2018b) surveyed multiple records and concluded with some skepticism that "if one considers the time-series of data according to their published chronologies, there is significant diachroneity of the event" and that "the duration of the event also differs significantly between records". With regard to the nature of the event, it was first recognized as a dry phase (e.g., Weiss et al., 1993) but has been reported in other settings as a wet phase (e.g., Li et al., 2018) or, in contrast to both, a time of variable conditions (Kathayat et al., 2017).

This range of responses suggests that careful definition of the various expressions of the event is needed. The event was first recognized as a dry phase in paleoclimatological data from the shores of southwestern Asia, specifically in the Gulf of Oman (Cullen et al., 2000) and the Red Sea (Arz et al., 2006), and its chronology has been most firmly established as extending, at least as a single event, from 4.26 ka to 3.97 ka (Carolin et al., 2019). Thus one might speak most strictly and surely of a "Southwest Asian 4.2 ka Dry Event" from 4.26 ka to 3.97 ka. Farther east and west, but in the same latitudinal zone from 20°N to 40°N, the event has been recognized as a dry event from central North American (Forman et al., 1995) to the Mediterranean (Drysdale et al., 2006) to the Himalayas (Nakamura et al., 2016) to Japan (Kawahata, 2019). However, that event is reported across a broader range of time and with some places in that latitudinal zone, such as southeastern China, wetter during that period (Zhang et al., 2018), suggesting a "Mid-latitude Northern Hemisphere ~4.2 ka Generally Dry Event". Recent work in the southern Hemisphere has suggested wetness around 4.2 ka (e.g., Li et al., 2018; Railsback et al., 2018b), suggesting a still-hypothetical "Southern Hemisphere Variably Wet 4.2 ka event". Most broadly, it appears that we will be forced to think of a "Globally Variable ~4.2 ka Event", in contrast to the seeming uniformity of the "global megadrought" of Weiss, (2016).

With the evolving context described above in mind, this paper returns to Dante Cave in northeastern Namibia, the site studied by Railsback et al. (2018b), to report further evidence for a wet 4.2 ka Event from two more stalagmites, DAN1 and DP2.

2. Setting

2.1. Physical setting

Dante Cave (19° 24′ S; 17° 53′ E) is developed in Proterozoic-age dolomitic bedrock of the Otavi Mountainland between the towns of Tsumeb and Grootfontein in the Otjozondjupa region of northeastern Namibia. It is accessed via a single vertical entrance, with a 9 m drop to a debris cone. Steep passages lead to chambers as much as 60 m below the land surface. Sletten et al. (2013), Voarintsoa et al. (2017a), and Railsback et al. (2019) provide more details of the physical setting of the cave.

2.2. Climate, moisture sources, and oxygen isotopes

Dante Cave is in southern Africa's region of summer rainfall, which is greatest in January and February, with about 120 mm each month. In July and August, on the other hand, virtually no rain falls, and June is also typically extremely dry. Temperatures range between an average of 26°C in December to 15.2°C in July. In the Köppen classification, the climate of the area is Bsh or hot arid steppe (Beck et al. 2018).

Rainfall in northern Namibia in January and February, and more generally in austral summer from November to March, occurs as the Tropical Rain Belt (Nicholson, 2018) migrates southward and/or westward in response to the annual increase in insolation in the Southern Hemisphere. Dante lies consistently south of the Inter-Tropical Convergence Zone (ITCZ), even in summer (Nicholson 2018), and in fact the ITCZ "remains well north of the equator" across Africa all year (Nicholson, 2018).

Dante has a more complicated relationship with the Congo Air Boundary (CAB), which marks the convergence of easterly winds from the Indian Ocean and cyclonic winds from the South Atlantic and Congo Basin. Several authors have suggested that the Congo Air Boundary (CAB) has a major impact on rainfall in southern Africa. However, assessing the importance of the CAB in bringing rainfall to Dante is difficult given considerable uncertainty as to its actual location during the austral spring and summer. Figure 1 illustrates the problem because, depending on author, the boundary varies from almost north to south through Botswana (Nicholson 1996, reproduced in Gasse 2000), to largely east to west near or north of the Angola-Namibia border (van Heerden and Taljaard 1998; Chase et al. 2009; Howard and Washington 2019).

Most recently, the nature of the CAB and its influence on southern African rainfall have been reassessed using the ERA-5 reanalysis dataset (Howard and Washington, 2019) in seemingly the first attempt "to identify the CAB in reanalysis datasets or in global or regional atmospheric models". In that study, the CAB maintained an ENE to WSW orientation while migrating southwards in austral spring and early summer (Aug to Dec) to a position in southern Angola and southern Zimbabwe. By December (the last month presented in Figs, 2, 4, and 10 of Howard and Washington, 2019), the CAB was still well north of the Angola-Namibia border and was beginning to break down (Fig. 1). A second boundary, the Kalahari discontinuity (KD), marked convergence between the trades and the southerly Namibian nocturnal low-level jet and became more prominent in November and December (Fig. 1). The KD was oriented northwest–southeast from northern Namibia into southwesternmost Botswana and formed the main humidity gradient in November and December as the CAB began to break down. Thus, one understanding of Fig. 1 is that diverse pre-2019 portrayals of the CAB were attempts to represent a synthesis of the CAB (in the strict sense of Howard and Washington, 2019) and the then-unrecognized KD.

Because the CAB and KD both divide hotter drier air to the south from moister and often saturated air to the north, both at the surface and aloft, they both have the potential to play a role in interannual variation in rainfall. In addition, breakdown of the CAB and strengthening of the easterlies can trigger the formation of tropical-temperate-troughs (TTTs), which are a major source of rainfall in subtropical southern Africa in summer. Howard and Washington (2019) noted that the early breakdown of the CAB often occurs when the low-level easterlies become more humid. As a result, breakdown of the CAB is often associated with increased rainfall from the Indian Ocean, with the flow of moist air southwards from the Congo, and with a strengthening and westward migration of the KD.

Breakdown of the CAB as a result of moister, easterly winds, before the convergence zone reaches Dante Cave, suggests that rainfall at the cave is derived largely from the east, not from the north. Indeed, the isotopic signature of the easterlies has dominated the O-isotope ratios in stalagmite $CaCO_3$ from northeastern South Africa to northeastern Namibia in the late Quaternary (Fig. 10 of Railsback et al. (2018a), suggesting a large continental effect during transport of vapor westward across southern Africa (see also Section 3.2). Thus, the KD and its weak moisture source from the easterlies may be the best explanation of the source of summer rain in the region around Dante Cave (Fig. 1).

3. Methods and criteria

3.1 Laboratory methods

The two stalagmites from which data are reported here were sectioned and polished along their growth axes, and chips measuring 5.0 cm by 7.5 cm were cut from which thin sections of the intervals near 4.2 kyr in age were prepared. Samples for radiometric dating and stable-isotope analysis were removed using dental burs and a dental handpiece. These samples were positioned so that they did not cross layer-bounding surfaces (Railsback et al., 2013, and Section 3.2 below). For determination of age, the samples were analyzed by use of a multi-collector inductively coupled plasma mass spectrometer (MC-ICPMS, Thermo-Finnigan Neptune) in the University of Minnesota's Department of Earth Sciences using methods described in Shen et al. (2002) and Cheng et al. (2013). The chemical procedure used for separation of U and Th was that of Edwards et al. (1987) and Shen et al. (2002). The initial results were corrected by assuming an initial $^{230}Th/^{232}Th$ atomic ratio of $4.4 \pm 2.2\times10^{-6}$, which is the value for a material at secular equilibrium with the bulk earth $^{232}Th/^{238}U$ value of 3.8. The resulting corrections ranged from 0 to 97 years, with a mean of 13.0 years.

For stable isotope analysis, samples of 50 to 100 μg each were analyzed on a GasBench-IRMS system at the Alabama Stable Isotope Laboratory using methods similar to those of Paul and Skrzypek (2007). The results were normalized using NBS-19, which has $\delta^{13}C$=1.95‰ relative to VPDB and $\delta^{18}O$=−2.20‰ relative to VPDB. The resulting isotope ratios are reported relative to the VPDB (Vienna Peedee Belemnite) standard.

X-ray diffraction of powdered samples was performed using a Bruker D8 X-ray Diffractometer in the Department of Geology of the University of Georgia by means of scans from 20 to 65° 2θ with $Co_{K\alpha}$ radiation.

3.2 Criteria for interpretation

The criteria used to identify the 4.2 ka Event in this project were Type E layer-bounding surfaces, as well as $\delta^{13}C$ data and $\delta^{18}O$ data (Figs. 2 and 3). A layer-bounding surface is a surface that cuts across multiple layers of a stalagmite, akin to an unconformity in the stratigraphy of sedimentary rocks. At Type E surfaces (Railsback et al., 2013), the underlying $CaCO_3$ has been removed, as evidenced by an irregular or jagged surface incised into that underlying $CaCO_3$. The origin of these surfaces is most readily understood as a change from dripwater supersaturated with respect to $CaCO_3$ to dripwater undersaturated with respect to $CaCO_3$. An alternate explanation might be physical abrasion, but this would likely lead to a polished smooth surface, rather than a jagged one. Furthermore, Type E surfaces are commonly coated with detrital clay, suggesting flowing or flooding rather than dripping water and thus an increase in water supply. Incision and coating combine to suggest more dilute and more abundant water, both of which would be expected in a change to conditions wetter than those during which the underlying spelean $CaCO_3$ was deposited. Inference of wetter conditions from the presence of Type E surfaces has been made by Perrin et al. (2014), Shtober-Zisu et al. (2014), Meckler et al. (2015), Martín-Chivelet (2017), Kenny (2018), Liu et al. (2019), López-Martinez (2020), and Fu et al. (2021).

Values of $\delta^{13}C$ in stalagmites are controlled by at least eight different contextual parameters (McDermott, 2004; Table 1 of Voarintsoa et al., 2017b, and sources cited therein). Some of these, such as $\delta^{13}C$ of the overlying limestone or the extent of Earth's glaciation, are unlikely to change during the deposition of a few layers in one stalagmite. The three contextual parameters most likely to change over short (~decadal) time spans are (1) the extent of vegetation and soil biomass productivity (where lower $\delta^{13}C$ occurs with more vegetation cover in response to wetter conditions) (Hesterberg and Siegenthaler, 1991), (2) the extent of prior precipitation of $CaCO_3$ from the drip water (where lower $\delta^{13}C$ occurs with less prior $CaCO_3$ precipitation typical of wetter conditions) (e.g., Johnson et al., 2006), and (3) the photosynthetic pathway of the overlying plant community. The last of these three is the most confounding, because (a) in wet to semi-arid environments the C3 plants dominant in wetter conditions generate lower values of $\delta^{13}C$, whereas (b) in semi-arid environments C4 plants typical of hotter, drier or summer-rain climates generate higher values of $\delta^{13}C$ (Vogel et al., 1978; Brook et al., 2010), but (c) in arid environments C4 grasses do not survive, leaving only C3 scrub as the vegetation, so that lower values of $\delta^{13}C$ are taken as evidence of drier conditions (e.g., Belz et al., 2020) – although the C3 scrub may be so limited that its production of low-$\delta^{13}C$ soil CO_2 is small and does not generate a noticeably low value of stalagmite $\delta^{13}C$.

Values of $\delta^{18}O$ in stalagmites are likewise controlled by at least eight different contextual parameters (McDermott, 2004; Lachniet, 2009; Table 1 of Voarintsoa et al., 2017b, and sources cited therein). Some of these, such as altitude of the cave or glacial-interglacial change of $\delta^{18}O$ of the oceans, are unlikely to change during the deposition of a few layers in one stalagmite. The contextual parameters most likely to change over short (~decadal) time spans are (1) amount of rainfall, where $\delta^{18}O$ commonly decreases with increasing rainfall (Dansgaard, 1964), (2) extent of evaporation of soil water or drip water, where $\delta^{18}O$ decreases with lesser evaporation in wetter conditions (Cuthbert et al. 2014), and (3) temperature, where $\delta^{18}O$ decreases with increasing temperature (McDermott, 2004; Lachniet, 2009). The first two parameters conspire to give lower $\delta^{18}O$ in wetter conditions, but decreasing temperature can confound that trend. Another contextual parameter relevant at Dante Cave is the distance that water vapor travels to a cave from its source, because greater distance allows more rain-out of ^{18}O and thus a lower $\delta^{18}O$ of the rainfall (the "continental effect"). However, as noted in Section 2.2, Dante's location under the shifting CAB and/or KD means that $\delta^{18}O$ of rainwater can change considerably, further confounding interpretation of $\delta^{18}O$ from spelean carbonates in the cave.

A very general summary of the previous two paragraphs is that lower values of $\delta^{13}C$ and $\delta^{18}O$ data are commonly interpreted as evidence of wetter conditions in wet to semi-arid environments (e.g., Section 5.1 of Sletten et al., 2013), but fallibly so. In the best case, a *slow* change to wetter conditions as suggested by the above general model results in lower values of $\delta^{18}O$ and $\delta^{13}C$ spanning a long time interval and thus across a significant vertical distance in the stalagmite, so that dissolution at peak wetness nonetheless leaves $CaCO_3$ bearing those lower values of $\delta^{18}O$ and $\delta^{13}C$ (Fig. 4A). However, a *rapid* shift to wetter conditions leaves only a vertically thin interval of $CaCO_3$ bearing lower values of $\delta^{18}O$ and $\delta^{13}C$, so that dissolution at peak wetness can remove the $CaCO_3$ that bore the lower values of $\delta^{18}O$ and $\delta^{13}C$ (Fig. 4B). Thus rapid shifts to wetter conditions may be recorded only by the Type E layer-bounding surfaces described in the first paragraph of this section.

4. Results

4.1. Stalagmite DAN1

Stalagmite DAN1 is 28 cm tall and has a "fencepost" shape that is offset at four points, the uppermost of which is 2.8 cm from the top (Fig. 2A). The interval of DAN1 deposited near 4.2 ka BP is, in a coincidence of numbers, 4.2-4.1 cm from the top of the stalagmite. X-ray diffraction of samples drilled 4.3 and 4.1 cm from the top of DAN1 indicates that these samples consist almost entirely of aragonite.

Ages from the upper third of Stalagmite DAN1 range from 5.2 to 3.4 ka (Supplementary Document 1). In the same interval of the stalagmite there is petrographic evidence of four surfaces of dissolution (Type E surfaces in the terminology of Railsback et al., 2013 discussed in Section 3.2) to suggest hiatuses that are 5.4, 4.32, 4.15, and 3.89 cm from the top of the stalagmite (Fig. 2C). The closely-spaced hiatal surfaces, between which only one or two ages could be generated, precluded construction of an age model by statistical methods that assume constant deposition (e.g., COPRA or OxCal) in the time range of interest near 4.2 ka (Fig. 2C). The most pronounced of the four hiatuses with regard to both petrographic characteristics and temporal duration is the one 4.15 cm from the top (it is in fact the most visible hiatal surface in the entire stalagmite). Petrographically it is distinguished by an undulating surface of corrosion overlain by a thick layer of fine detrital material, presumably clay, with sand-sized carbonate particles and at least one piece of phosphatic debris that may be a fragment of bone (Fig. 2B). It is by far the most pronounced surface of dissolution and detrital deposition in Stalagmite DAN1. Values of $\delta^{13}C$ are low around the surface and lowest just below it (Fig. 2D), giving the largest excursion in $\delta^{13}C$ in the entire stalagmite).

Chronologically, the Type E surface at 4.15 cm from the top of Stalagmite DAN1 represents a gap of 300 to 400 years that presumably represents (a) time lost from the record because underlying $CaCO_3$ was dissolved (giving the earlier part of the hiatus) and (b) time when $CaCO_3$ was not deposited during that dissolution and during deposition of the detrital material (giving the later part of the hiatus) (Fig. 2). The best estimate of the latter, the time of erosion (presumably by dissolution), and of deposition of detrital material (presumably by flowing water), is from 4.1 to 3.9 ka BP (Fig. 2C), which falls within the time range that Railsback et al. (2018b) in their Figs. 2 and 3 found was compatible with eleven previously published chronologies of the 4.2 ka Event.

4.2. Stalagmite DP2

Stalagmite DP2 is 37 cm tall and has a nearly perfect fencepost shape (Fig. 3A). The interval of DP2 deposited near 4.2 ka BP is 33-34 cm from the top, and thus near the stalagmite's base. X-ray diffraction of samples drilled 33 and 34 cm from the top of DP2 indicates that those samples consist entirely of aragonite, although a very thin interval (too thin to sample for X-ray diffraction) has the petrographic characteristics of calcite (Fig. 3B).

The most prominent feature of Stalagmite DP2 is a thin detrital layer low in the stalagmite, 334 mm from the top. Microscopic examination reveals that this detrital layer overlies a surface of corrosion that is also overlain by spelean calcite, in contrast to the aragonite otherwise present above and below the detrital layer (Fig. 3B). This Type E surface is easily the most visible hiatal surface in the entire stalagmite. Values of both $\delta^{18}O$ and $\delta^{13}C$ below the detrital layer deviate in the negative direction from the otherwise upward-increasing trend, but the negative anomaly in both cases is only 0.3‰.

The exact age of the detrital layer 334 mm from the top of Stalagmite DP2 is uncertain because U-Th ages are inconsistent near the base of the stalagmite. Five ages support an age model readily generated by interpolation yielding an age of 4080 to 4040 yrs BP for the layer

(Case α in Fig. 3C), two ages support an age model necessarily generated by interpolation yielding an age of 4340 to 4300 yrs BP (Case β in Fig. 3C), while an age model that is a compromise between all seven ages yields an age of 4210 to 4150 yrs BP (Case γ in Fig. 3C). All three model ages for the detrital layer fall within the time range of anomalies elsewhere that have been ascribed to the 4.2 ka Event (e.g., Zanchetta et al., 2016). More importantly, the age of 4080 to 4040 yrs BP suggested by Case α, which is the age model based on the largest number of U-Th ages, falls within the time range that Railsback et al. (2018b) in their Figs. 2 and 3 found was compatible with eleven previously published chronologies of the 4.2 ka Event (Booth et al., 2004; Drysdale et al., 2006; Lemcke and Sturm, 1997; Kaufmann et al., 1988; Berkelhammer et al., 2012; Staubwasser et al., 2003; Cullen et al., 2000; Arz et al., 2006; Sharifi et al., 2015; Kröpelin et al., 2008; Ohlendorf et al., 2014).

5. Discussion

5.1. Inferences from Stalagmites DAN1 and DP2

Stalagmite-based studies of past climate range from those using multiple proxies of past climate (e.g., Scholz et al., 2012; Carolin et al., 2019) to those using just one proxy, typically $\delta^{18}O$ (e.g., Cheng et al., 2011; Kathayat et al., 2017). Researchers employing multiple proxies presumably do so in hope that meaningful inferences can be made from the synthesis of multiple lines of evidence and/or in hope that, if one proxy fails to record an event or trend, others will nonetheless provide evidence of an otherwise missed paleoclimatological phenomenon. This paper follows that model in reporting five kinds of data or evidence: $\delta^{18}O$, $\delta^{13}C$, layer-bounding surfaces, detrital content, and mineralogy of $CaCO_3$.

The Type E surfaces in Stalagmites DAN1 and DP2 are evidence of dissolution that requires undersaturated waters passing over the stalagmite. Values of $\delta^{18}O$ show only the slightest of decreases below the Type E surface in Stalagmite DP2 and none in Stalagmite DAN1.

However, as Fig. 4 shows, abrupt change to conditions sufficiently wet to cause stalagmite dissolution (and thus a Type E surface) is likely to remove the $\delta^{18}O$ signal of that rapid change to wetter conditions. Thus absence of a low-$\delta^{18}O$ excursion is not necessarily an argument against a trend to wetter conditions, and in fact monotonous $\delta^{18}O$ values below a hiatal Type E surface suggest *abruptly* wetter conditions (Fig. 4). The expression "abrupt change" is relevant here because the 4.2 ka Event has been widely regarded as an example of abrupt climate change (Rashid and Polyak, 2011; Zhang et al., 2018; Carolin et al., 2019; Pleskot et al., 2019; Ön et al., 2021).

In light of the previous paragraph, one logical approach is to use the method of multiple working hypotheses (Chamberlin, 1890). Here we consider five hypotheses regarding the paleoclimatological implications of the Type E surfaces and associated geochemical evidence dating to roughly 4.2 ka from Stalagmites DAN1 and DP2:

Hypothesis 1: Nothing anomalous took place. In each stalagmite, three things (the hiatus apparent in the age model, the presence of a corroded surface more pronounced than any other in the stalagmite, and the accumulation of detrital material in an otherwise much cleaner stalagmite) combine to document *some* anomalous event. This hypothesis is therefore disproven.

Hypothesis 2: An unusually wet event or period took place. Three lines of evidence support this hypothesis. (i) In each stalagmite, accumulation of detrital material in an otherwise much cleaner stalagmite supports passage of a large flux of water sufficient to transport solids. Such material may have been deposited either from an exceptionally large flux of falling water or by flooding of the cave and submergence of the stalagmite. In either case, the fact that the accumulations of detrital material reported here are the most pronounced such accumulations in their respective stalagmites suggests that they represent the wettest conditions, either as descending water, flood water, or both, during those stalagmites' centuries to millennia of deposition. (ii) In each stalagmite, presence of a corroded (Type E) surface more pronounced than any other in the stalagmite supports a wet event. The truncation of underlying calcite at irregular surfaces indicates dissolution, rather than the deposition that otherwise generates a stalagmite. Dissolution in turn implies fluxes of undersaturated groundwater through the regolith and bedrock over the cave, and their passage into the cave so rapidly that the water had no time to degas and reach saturation. (iii) In Stalagmite DP2, the change in precipitation from aragonite to calcite is also consistent with wetter conditions (Railsback et al., 1994, and sources cited therein). Thus *three* lines of evidence (detrital content, dissolution, and mineralogy) support an unusually wet event or period.

Hypothesis 3: An unusually dry event or period took place. Evidence of a dry event in a stalagmite typically consists of a shift of $\delta^{18}O$ to greater values (see Section 3.2), a shift of $\delta^{13}C$ to greater values (see Section 3.2), a thinning of layers, and/or a lessening of the area at the top of the stalagmite covered by those layers (a Type L surface in the jargon of Railsback et al., 2013). None of this evidence is present, and so the hypothesis is not supported.

Hypothesis 4: An unusually wet event was followed by an unusually dry event. As noted with regard to Hypothesis 3, there is no evidence of a dry event, and so the hypothesis is not supported.

Hypothesis 5: An unusually dry event was followed by an unusually wet event. As noted with regard to Hypothesis 3, there is no evidence of a dry event, and so the hypothesis is not supported.

Of these five hypotheses, only Hypothesis 2 (an unusually wet event or period) is supported by the available evidence. Hypotheses 4 and 5 are possible, but there is no evidence to support the "dry" components of these hypotheses.

The understanding of detrital material presented above assumes that water routinely moving at very slow rates in the pathways to drips does not have kinetic energy sufficient to carry suspended solids, especially solids as large as the sand-sized grains reported above. In this view, such suspended solids would only accompany exceptionally rapid flow, and the presence of such solids at the crests of stalagmite layers would be evidence of exceptionally wet conditions, either with gushing "drip" water onto the stalagmite or rising standing water around the stalagmite. An alternate understanding might be that cave drips, despite their clarity and slow movement, in fact routinely carry suspended solids (Yadava et al., 2004) as large as fine sand and routinely deliver these to the crests of stalagmites, where greater flow washes the solids off the crests and lesser flow allows the solids to remain. In this view, a drying trend would be indicated by migration of a detritus-rich zone upward through layers/time from the flanks of stalagmite to its crest (Fig. 5). This pattern is not observed in Stalagmites DAN1 and DP2, and thus the drying trend suggested by Hypotheses 3 to 5 above is not supported. Furthermore, Yadava et al. (2004) wrote of "fine detritus", not sand-sized grains like those shown in Fig. 2B.

5.2. The combined data from Stalagmites DAN1, DP2, and DP1

The evidence from Stalagmites DAN1 and DP2 reported here combines with evidence from Stalagmite DP1 reported by Railsback et al. (2018b) to give *three* stalagmites from Dante Cave indicating anomalously wet conditions during the 4.2 ka Event in northeastern Namibia. (A Type E surface and C and O stable isotope data from Stalagmite DP1 were also the evidence of a wet phase in that stalagmite's record). Paleoclimatological research using stalagmites commonly must be defended from claims of non-replication among the stalagmites themselves (as in Section 3.3 of Sletten et al., 2013) or with other data (Betancourt et al., 2002), but in this case the only three stalagmites from Dante Cave known to span the time of the 4.2 ka Event all provide evidence of the same wet paleoclimatological anomaly.

5.3. Other proxy evidence of a wet 4.2 ka Event in Namibia and Botswana

There are many proxy records of Holocene climate from northwestern Botswana and northern Namibia, as shown by Fig. 1 of Burrough and Thomas (2013) and Fig. 4 of De Cort et al. (2021), although not all records are of sufficiently high chronological resolution to recognize an abrupt climate event like the 4.2 ka Event. One high-resolution record from the region is that of Chase et al. (2009), who used $\delta^{15}N$ and $\delta^{13}C$ data from hyrax middens from the Spitzkoppe inselberg in western-central Namibia (21.8°S, 15.2°E) to estimate change between wetter and drier conditions during the Holocene. Their data (Fig. 6D) show a short-term minimum in $\delta^{15}N$ (and thus a maximum of wetness of climate) and short-term maximum in $\delta^{13}C$ (and similarly a maximum in wetness in Spitzkoppe's xeric conditions) in which the most negative single $\delta^{15}N$ measurement dates to 4067 BP, at essentially the best estimate of the timing of the 4.2 ka Event (Railsback et al., 2018b, Figs. 2 and 3). That $\delta^{15}N$ measurement is at the apex of a broader $\delta^{15}N$ minimum from 4223 to 4005 yrs BP matching the time of the 4.2 ka Event in the "precise timing" of the main pulse of the 4.2 ka Event in the Middle East at 4.28 to 3.97 ka BP by Carolin et al. (2019, their Fig. 4). The $\delta^{13}C$ data from Spitzkoppe similarly have a multi-point maximum that matches the time of the 4.2 ka Event as inferred by Carolin et al. (2019) (Fig. 5D). The data of Chase et al. (2009) thus join the evidence from the three stalagmites from Dante Cave in indicating wetness in Namibia during the 4.2 ka Event.

Two records extending from the latest Pleistocene to the Holocene and thus of somewhat lower resolution are those of Cordova et al. (2017) and Belz et al. (2021) (Fig. 7). Cordova et al. (2017) used pollen, spore, and charcoal data to produce a reconstruction of PWetQ (precipitation in the wettest quarter) at Lake Ngami in northwestern Botswana. That reconstruction has a broad maximum at 4.0 ka compatible with a wet 4.2 ka Event at Lake Ngami, although the chronological uncertainty of the record is considerable (Fig. 7A). To the west of that location, at Omongwa Pan in eastern Namibia, Belz et al. (2020) used stable-isotope data to study past climate. Their record of $\delta^{13}C$ of total organic carbon (TOC) in sediments there has a minimum followed immediately by a maximum (suggesting exceptional dryness followed abruptly by exceptional wetness) in the interval from 4.2 to 3.7 ka. (Fig. 7B) However, the chronological uncertainty of that record is even greater, so that one could infer either exceptional wetness or exceptional dryness in the 4.2 ka event, which most likely occurred around 4.1 ka (Railsback et al., 2018; Carolin et al., 2019). The result is that the records of both Cordova et al. (2017) and Belz et al. (2021) are compatible with (but do not conclusively support) a wet 4.2 ka Event in northwestern Botswana and eastern Namibia and thus are compatible with the inferences of this paper.

5.4. Other proxy evidence of a wet 4.2 ka Event in the Southern Hemisphere

Since the first explicit report of evidence of a wet 4.2 ka Event in the Southern Hemisphere (Railsback et al., 2018a), Li et al. (2018) have reported evidence of wetness during the 4.2 ka Event in a stalagmite from Rodrigues Island (19° 42' S, 63° 24' E) in the southern Indian Ocean. Most specifically, both their $\delta^{18}O$ and $\delta^{13}C$ data suggest a wet pulse at about 4115 yrs BP, or more broadly from 4130 to 4020 yrs BP (Fig. 6B).

In their Fig. 4, Li et al. (2018) also compiled isotopic evidence of wetness during the 4.2 ka Event at five other locations in and around the Indian Ocean. Since their work, Li et al. (2020) have additionally reported evidence of wetness during the 4.2 ka Event on Amsterdam Island in the southern Indian Ocean (Fig. 8). Even farther afield, Yan and Liu (2019) noted that Marchant and Hooghiemstra (2004) had inferred a rise in the level of Lake Titicaca (12.08°S, 69.85°W) around 4.0 ka (Fig. 8). These reports combine to suggest that many regions of the Southern Hemisphere may have had relatively wet climatic excursions during the 4.2 ka Event. In addition, Zhang et al. (2018) reported that $\delta^{18}O$ and $\delta^{13}C$ data from southern China suggest a wet 4.2 ka Event, and Tan et al. (2018) likewise reported evidence of generally wetter conditions in southern China than in northern China during the 4.2 ka Event. These reports combine to suggest that many (but not all) regions, especially in the Southern Hemisphere, may have had relatively wet climatic excursions during the 4.2 ka Event.

5.5. Comparison with modeling studies, ITCZ, and AMOC

Yan and Liu (2019) used TraCE-21ka (Simulation of Transient Climate Evolution over the past 21,000 years) simulated using the Community Climate System Model Version 3 (CCSM3) to investigate the geographic variability of temperature and rainfall during the 4.2 ka Event. Specifically, Yan and Liu (2019) looked at characteristics between NH warm/wet and cold/dry centennial events found in the 5-3 ka window of a 21ka transient simulation. They found two troughs between 4.4 to 4.0 ka in the annual mean NH surface temperature (down to -0.18 °C from the 5-3 ka mean) and annual mean NH precipitation (down to maximum -0.2 mm/day) simulated timeseries. They also found similar-to-larger amplitude peaks in NH T and P from 4.8-4.5 ka and from 4.0-3.85 ka. To discuss potential spatial characteristics of a 4.2 ka NH cold/dry event, Yan and Liu (2019) plotted spatially the difference in various climate parameters between the 2 centennial NH cold/dry periods and the 2 centennial NH warm/wet periods of the 5-3 ka window.

Figure 3B of Yan and Liu (2019) suggests cooling everywhere north of 50°N and nearly everywhere north of 10°S. The modeled precipitation is also latitudinally dependent, but less strikingly so, in suggesting drying everywhere north of 75°N, general drying with lesser regions of increased moisture from 75°N to 5°N, and mixed responses southward from 5°N. The most striking region of increased moisture, with regard to both amount (as much as 70-80 mm/yr) and higher confidence level, was in the zone from the Equator to 35°S (Fig. 8). Yan and Liu concluded that the patterns in temperature and precipitation were consistent with a southward shift in the ITCZ, as had been suggested by Railsback et al. (2018) and Zhang et al. (2018) and more generally is consistent with the findings of Schefuß et al. (2011) regionally and Chiang and Friedman (2012) globally.

Figure 8 shows that many of the locations of proxy evidence of a wet 4.2 ka Event discussed in Section 5.4 lie in the regions of wetter conditions at 4.2 ka inferred by Yan and Liu (2019). One should note that this is not just a matter of proxy locations in the Southern

Hemisphere and general wetting in the Southern Hemisphere. For example, of two proxies of climate change in South America, the one suggesting increased moisture at Lake Titicaca lies in Yan and Liu's general zone of more rainfall from the Equator to 35°S, whereas evidence of drying at Laguna Cháltel lies in their latitudinal belt of diminished rainfall from 40° to 50°S. Furthermore, this linkage of a wet 4.2 ka Event to ITCZ migration is evident not only in the Southern Hemisphere but also in the Northern Hemisphere: Zhang et al. (2018) and Tan et al. (2018) concluded that the wet 4.2 ka Event in southern China resulted from a southward shift of the ITCZ, so that the East Asian Monsoon did not advance into northern China and instead delivered rainfall to southern China. That short-term observation is consistent with the long-term finding by An et al. (2001) that the region of greatest monsoonal wetness moved from north to south in China across the entire Holocene as the Northern Hemisphere cooled. The abrupt southward shift of the ITCZ around 4.1 ka BP has been attributed to weakening of the Atlantic Meridional Overturning Circulation (AMOC) (Zhang et al., 2018; Yan and Liu, 2019; Geirsdóttir et al., 2019), which brings heat to the Northern Hemisphere.

6. Conclusions

New observations from two previously unreported stalagmites from Dante Cave in northeastern Namibia are most compatible with an inference of a wet phase at 4.2-3.9 ka; consideration of multiple hypotheses in fact shows that wetness during the 4.2 ka Event is the only hypothesis supported by the available evidence. These observations combine with previous results from a third Dante stalagmite to indicate wetness, rather than drought, during the 4.2 ka Event. These data from Dante Cave add to a growing body of evidence from eight locations in the Southern Hemisphere and others in southern China suggesting a wet 4.2 ka Event. Supporting the terrestrial data are recent modeling results that suggest zones of increased wetness during the 4.2 ka Event that covered much of the low-to-mid-latitude Southern Hemisphere and more limited regions of the Northern Hemisphere as the ITCZ migrated southward. It thus seems that the 4.2 ka Event cannot be taken to be a global episode of drying as previously suggested but instead must be viewed as a more diverse and complex interval with some areas wetter and some drier with a broad but imperfect latitudinal zonation. Both modeling and proxy data suggest that at least some (but not all) latitudinal zones in the Southern Hemisphere experienced wetter climate.

Declaration of competing interest

The authors declare that they have no known competing financial interests or personal relationships that could have appeared to influence the work reported in this paper.

Acknowledgements

Funding for this research came from U.S. National Oceanic and Atmospheric Administration (NOAA) grant NA56GP0325 to Brook, Railsback, Jean-Claude Thill and Richard S. Meltzer and from US National Science Foundation (NSF) grant 9908415 to Brook and Railsback. Brook and Eugene Marais collected Stalagmite DAN1 while Ben Hardt and Eugene Marais collected Stalagmite DP2. Dr. Irka Schüller of the Senckenberg am Meer, Marine Research Department in Wilhelmshaven, Germany, provided invaluable help with regard to the age data shown in Fig. 7. P3 Editor Paul Hesse, Reviewer Stacy Carolin, and three anonymous reviewers provided comments that greatly improved the manuscript.

References

An, Z., Porter, S.C., Kutzbach, J.E., Wu, X., Wang, S., Liu, X., Li, X., Zhou, W., 2000. Asynchronous Holocene optimum of the East Asian monsoon. Quaternary Science Reviews 19, 743–762.

Arz, H.W., Lamy, F., Pätzold, J., 2006. A pronounced dry event recorded around 4.2 ka in brine sediments from the northern Red Sea. Quaternary Research 66, 432–441.

Baldini, J.U.L., McDermott, F., Baker, A., Baldini, L.M., Mattey, D.P., Railsback, L.B., 2005. Biomass effects on stalagmite growth and isotope ratios: a 20th century analogue from Wiltshire, England. Earth and Planetary Science Letters 240, 486–494.

Bar-Matthews, M., Ayalon, A., Kaufman, A., Wasserburg, G.J., 1999. The Eastern Mediterranean paleoclimate as a reflection of regional events: Soreq cave, Israel. Earth and Planetary Science Letters 166, 85–95.

Belz, L., Schüller, I., Wehrmann, A., Köster, J., Wilkes, H., 2020. The leaf wax biomarker record of a Namibian salt pan reveals enhanced summer rainfall during the Last Glacial-Interglacial Transition. Palaeogeography, Palaeoclimatology, Palaeoecology 543, 109561.

Berkelhammer, M., Sinha, A., Stott, L., Cheng, H., Pausata, F.S.R., Yoshimura, K., 2012. An abrupt shift in the Indian Monsoon 4000 years ago. In: Giosan, L. (Ed.), Climates, Landscapes, and Civilizations: American Geophysical Union Monograph, vol. 198, pp. 75–87.

Betancourt, J.L., Grissino-Mayer, H.D., Salzer, M.W., Swetnam, T.W., 2002. A test of "Annual Resolution" in stalagmites using tree rings. Quaternary Research 58, 197–199.

Bini, M., Zanchetta, G., Perşoiu, A., Cartier, R., Català, A., Cacho, I., Dean, J. R., Di Rita, F., Drysdale, R. N., Finnè, M., Isola, I., Jalali, B., Lirer, F., Magri, D., Masi, A., Marks, L., Mercuri, A. M., Peyron, O., Sadori, L., Sicre, M.-A., Welc, F., Zielhofer, C., and Brisset, E.: The 4.2 ka BP Event in the Mediterranean region: an overview, Clim. Past, 15, 555–577, https://doi.org/10.5194/cp-15-555-2019, 2019.

Booth, R.K., Jackson, S.T., Gray, C.E.D., 2004. Paleoecology and high-resolution paleohydrology of a kettle peatland in Upper Michigan. Quat. Res. 61, 1–13.

Brook, G.A., Scott, L., Railsback, L.B., Goddard, E.A., 2010. A 35 ka pollen and isotope record of environmental change along the southern margin of the Kalahari from a stalagmite and animal dung deposits in Wonderwerk Cave, South Africa. Journal of Arid Environments 74, 870–884.

Burrough, S.L., Thomas, D.S.G., 2013. Central southern Africa at the time of the African Humid Period: a new analysis of Holocene palaeoenvironmental and palaeoclimate data. Quaternary Science Reviews 80, 29–46.

Carolin, S.A., Walker, R.T., Day, C.C., Ersek, V., Sloan, R.A., Dee, M.W., Talebian, M., Henderson, G.M., 2019. Precise timing of abrupt increase in dust activity in the Middle East coincident with 4.2 ka social change. Proceedings of the National Academy of Sciences 116, 67–72.

Chamberlin, T.C., 1890. The method of multiple working hypotheses. Science (old series), 15, 92-96.

Chase, B.M., Meadows, M.E., Scott, L., Thomas, D.S.G., Marais, E., Sealy, J., Reimer, P.J., 2009. A record of rapid Holocene climate change preserved in hyrax middens from southwestern Africa. Geology 37, 703–706.

Cheng, H., Zhang, P.Z., Spötl, C., Edwards, R.L., Cai, Y.J., Zhang, D.Z., Sang, W.C., Tan, M., An, Z.S., 2011. The climatic cyclicity in semiarid-arid central Asia over the past 500,000 years. Geophysical Research Letters 39, L01705.

Cheng, H., Edwards, R.L., Shen, C.C., Polyak, V.J., Asmerom, Y., Woodhead, J., Hellstrom, J., Wang, Y.J., Kong, X.G., Spötl, C., Wang, X.F., Alexander, E.C., 2013. Improvements in ^{230}Th dating, ^{230}Th and ^{234}U half-life values, and U-Th isotopic measurements by multi-collector inductively coupled plasma mass spectrometry. Earth and Planetary Science Letters 371, 82–91.

Chiang, J.C.H., Friedman, A.R., 2012. Extratropical cooling, interhemispheric thermal gradients, and tropical climate change. Annual Review of Earth and Planetary Sciences 40, 383–412.

Cordova, C.E., Scott, L., Chase, B.M., Chevalier, M., 2017. Late Pleistocene-Holocene vegetation and climate change in the Middle Kalahari, Lake Ngami, Botswana. Quaternary Science Reviews 171, 199–215.

Cullen, H.M., deMenocal, P.B., Hemming, S., Hemming, G., Brown, F.H., Guilderson, T., Sirocko, F., 2000. Climate change and the collapse of the Akkadian Empire: evidence from the deep sea. Geology 28, 379–382.

Cuthbert, M.O., Baker, A., Jex, C.N., Graham, P.W., Treble, P.C., Anderson, M.S., Acworth, R.I., 2014. Drip water isotopes in semi-arid karst: Implications for speleothem paleoclimatology. Earth and Planetary Science Letters 395: 194–204.

Dang, S., Yu, K., Tao, S., Han, T., Zhang, H., Jiang, W., 2020. El Niño/Southern Oscillation during the 4.2 ka event recorded by growth rates of corals from the North South China Sea. Acta Oceanologica Sinica. 39**,** 110–117. https://doi-org.proxy-remote.galib.uga.edu/10.1007/s13131-019-1520-5

Dansgaard, W., 1964. Stable isotopes in precipitation. Tellus 16, 436-468.

De Cort, G., Chevalier, M., Burrough, S.L., Chen, C.Y., Harrison, S.P., 2021. An uncertainty-focused database approach to extract spatiotemporal trends from qualitative and discontinuous lake-status histories. Quaternary Science Reviews 258, 106870.

Denniston, R. F., Wyrwoll, K. H., Polyak, V. J., Brown, J. R., Asmerom, Y., Jr, A. D.W., Lapointe, Z., Ellerbroek, R., Barthelmes, M., Cleary, D., 2013. A stalagmite record of Holocene Indonesian–Australian summer monsoon variability from the Australian tropics. Quaternary Science Reviews 78, 155–168.

Drysdale, R., Zanchetta, G., Hellstrom, J., Maas, R., Fallick, A., Pickett, M., Cartwright, I., Piccini, L., 2006. Late Holocene drought responsible for the collapse of Old World civilizations is recorded in an Italian cave flowstone. Geology 34, 101–104.

Edwards, R.L., Chen, J.H., Wasserburg, G.J., 1987. U-238 U-234-Th-230-Th-232 systematics and the precise measurement of time over the past 500,000 years. Earth and Planetary Science Letters 81, 175–192.

Forman, S., Oglesby, R., Markgraf, V., and Stafford, T., 1995. Paleoclimatic significance of Late Quaternary eolian deposition on the Piedmont and High Plains, Central United States. Global and Planetary Change, 11, 35–55, 1995.

Fu, R.R., Hess, K., Jaqueto, P., Novello, V.F., Kukla, T., Trindade, R.I.F., Stríkis, N.M., Cruz, F.W., Jr., Dor, O.B., 2021. High-resolution environmental magnetism using the quantum diamond microscope (QDM): application to a tropical speleothem. Frontiers in Earth Science 8, 604505.

Gasse, F., 2000. Hydrological changes in the African tropics since the Last Glacial Maximum. Quaternary Science Reviews 19, 189–211.

Geirsdóttir, A., Miller, G.H., Andrews, J.T., Harning, D.J., Anderson, L.S., Florian, C., Larsen, D.J., Thordarson, T., 2019. The onset of neoglaciation in Iceland and the 4.2 ka event. Climate of the Past 15, 25–40.

Giesche, A., Staubwasser, M., Petrie, C.A., Hodell, D.A., 2019. Indian winter and summer monsoon strength over the 4.2 kaBP event in foraminifer isotope records from the Indus River delta in the Arabian Sea. Climate of the Past 15, 73–90.

Griffiths, M. L., Drysdale, R. N., Gagan, M. K., Zhao, J. X., Ayliffe, L. K., Hellstrom, J. C., Hantoro, W. S., Frisia, S., Feng, Y. X., and Cartwright, I., 2009. Increasing Australian-Indonesian monsoon rainfall linked to early Holocene sea-level rise, Nature Geoscience, 2, 636– 639.

Hesterberg, R., Siegenthaler, U., 1991. Production and stable isotope composition of CO_2 in a soil near Bern, Switzerland. Tellus 43B, 197–205.

Howard, E., Washington, R., 2019, Drylines in southern Africa: rediscovering the Congo Air Boundary. Journal of Climate 32, 8223-8242.

Hutton, J., 1788. Theory of the Earth; or an Investigation of the Laws Observable in the Composition, Dissolution, and Restoration of Land upon the Globe. Transactions of the Royal Society of Edinburgh 1, 209–304.

Johnson, K.R., Hu, C.Y., Belshaw, N.S., Henderson, G.M., 2006. Seasonal trace-element and stable-isotope variations in a Chinese speleothem: the potential for high-resolution paleomonsoon reconstruction. Earth Planet. Sci. Lett. 244, 394–407.

Kathayat, G., Cheng, H., Sinha, A., Yi, L., Li, X., Zhang, H., Li, H., Ning, Y., Ning, Y., Edwards, R. L., 2017. The Indian monsoon variability and civilization changes in the Indian subcontinent. Science Advances 3, e1701296.

Kathayat, G., Cheng, H., Sinha, A., Berkelhammer, M., Zhang, H., Duan, P., Li, H., Li, X., Ning, Y., Edwards, R. L., 2018. Evaluating the timing and structure of the 4.2 ka event in the Indian summer monsoon domain from an annually resolved speleothem record from Northeast India, Climate of the Past, 14, 1869–1879.

Kaufman, A., Wasserburg, G.J., Porcelli, D., Bar-Matthews, M., Ayalon, A., Halicz, L., 1988. U–Th isotope systematics from the Soreq cave, Israel and climatic correlations, Earth and Planetary Sciences Letters 156, 141–155.

Kawahata, H., 2019. Climatic reconstruction at the Sannai-Maruyama site between Bond events 4 and 3-implication for the collapse of the society at 4.2 ka event. Progress in Earth and Planetary Science 6, 63.

Kenny, R., 2019. Stable isotope ratios and speleothem chronology from a high-elevation alpine cave, southern San Juan Mountains, Colorado (USA): Evidence for substantial deglaciation as early as 13.5 ka. AIMS Geosciences, 5, 41–65.

Kröpelin, S., Verschuren, D., Lézine, A.-M., Eggermont, H., Cocquyt, C., Francus, P., Cazet, J.-P., Fagot, M., Rumes, B., Russell, J.M., Darius, F., Conley, D.J., Schuster, M., von Suchodoletz, H., Engstrom, D.R., 2008. Climate-driven ecosystem succession in the Sahara: the past 6000 years. Science 320, 765–768.

Lachniet, M.S., 2009. Climate and environmental controls on speleothem oxygen isotope values. Quaternary Science Reviews. 28, 412–432.

Lemcke, G., Sturm, L., 1997. $\delta^{18}O$ and trace element measurements as proxy for the reconstruction of climate changes at Lake Van (Turkey): preliminary results. In: Dalfes, H.N., Kukla, G., Weiss, H. (Eds.), Third Millennium BC Climate Change and Old World Collapse: NATO ASI Series, vol. 149, pp. 653–678.

Li, H., Cheng, H., Sinha, A., Kathayat, G., Spötl, C., André, A.A., Meunier, A., Biswas, J., Duan, P., Ning, Y., Edwards, R.L., 2018. Hydro-climatic variability in the southwestern Indian Ocean between 6000 and 3000 years ago. Climate of the Past 14, 1881–1891.

Li, C., Sonke, J.E., Le Roux, G., Van der Putten, N., Piotrowska, N., Jeandel, C., Mattieli, N., Benoit, M., Wiggs, G.F.S., De Vleeschouwer, F., 2020. Holocene dynamics of the southern westerly winds over the Indian Ocean inferred from a peat dust deposition record. Quaternary Science Reviews 231, 106169.

Liu, D., Liu, S., Fang, Y., 2019. A southern and northern control on speleothem-based Asian summer monsoon variability during MIS 4. Quaternary Research 92, 738–753.

Liu, F., Feng, Z., 2012. A dramatic climatic transition at ~4000 cal. yr BP and its cultural responses in Chinese cultural domains. Holocene 22, 1181–1197.

López-Martínez, R., Gázquez, F., Calaforra, J.M., Audra, P., Bigot, J.Y., Puig, T.P., Alcántara-Hernández, R.J., Navarro, A., Crochet, P., Martínez, L.C., Brunet, R.D., 2020. Bubble trail and folia in cenote Zapote, México: petrographic evidence for abiotic precipitation driven by CO_2 degassing below the water table. International Journal of Speleology 49, 173–186.

Marchant, R. and Hooghiemstra, H., 2004. Rapid environmental change in African and South American tropics around 4000 years before present: a review. Earth-Science Reviews, 66, 217–260.

Martín-Chivelet,, J., Muñoz-García, M.B., Cruz, J.A., Ortega, A.I., Turrero, M.J., 2017. Speleothem Architectural Analysis: Integrated approach for stalagmite-based paleoclimate research. Sedimentary Geology 353, 28–45.

McDermott, F., 2004. Palaeo-climate reconstruction from stable isotope variations in speleothems: a review. Quaternary Science Reviews 23, 901–918.

Meckler, A.N., Affolter, S., Dublyansky, Y.V., Kruger, Y., Vogel, N., Bernasconi, S.M., Frenz, M., Kipfer, R., Leuenberger, M., Spotl, C., Carolin, S., Cobb, K.M., Moerman, J., Adkins, J.F., Fleitmann, D., 2015. Glacial-interglacial temperature change in the tropical West Pacific: A comparison of stalagmite-based paleo-thermometers. Quaternary Science Reviews 127, 90-116.

Nakamura, A., Yokoyama, Y., Maemoku, H., Yagi, H., Okamura, M., Matsuoka, H., Miyake, N., Osada, T., Adhikari, D.P., Dangol, V., Ikehara, M., Miyari, Y., Matsizaki, H., 2016. Weak monsoon event at 4.2 ka recorded in sediment from Lake Rara, Himalayas. Quaternary International 397, 349–359.

Nicholson, S.E., 1996. A review of climate dynamics and climate variability in eastern Africa. In: Johnson, T.C., Odado, E.O. (Eds.), Limnology, Climatology, and Paleoclimatology of the East African Lakes, pp. 25-56.

Nicholson, S.E., 2018. The ITCZ and the seasonal cycle over equatorial Africa. Bulletin of the American Meteorological Society 99, 337–348.

Ohlendorf, C., Fey, M., Massaferro, J., Haberzettl, T., Laprida, C., Lücke, A., Maidana, N., Mayr, C., Oehlerich, M., Marcau, J.R., Wille, M., Corbella, H., St-Onge, G., Sch€abitz, F., Zolitschka, B., 2014. Late Holocene hydrology inferred from lacustrine sediments of Laguna Cháltel (southeastern Argentina). Palaeogeography Palaeoclimatology Palaeoecology 411, 229–248.

Ön, Z.B., Greaves, A.M., Akçer-Ön, S., Özeren, M.S., 2021. A Bayesian test for the 4.2 ka BP abrupt climatic change event in southeast Europe and southwest Asia using structural time series analysis of paleoclimate data. Climatic Change 165, 7.

Park, J., Park, J., Yi, S., Kim, J.C., Lee, E., Choi, J., 2019. Abrupt Holocene climate shifts in coastal East Asia, including the 8.2 ka, 4.2 ka, and 2.8 ka BP events, and societal responses on the Korean peninsula. Scientific Reports 9:10806.

Paul, D., Skrzypek, G., 2007. Assessment of carbonate-phosphoric acid analytical technique performed using GasBench II in continuous flow isotope ratio mass spectrometry. International Journal of Mass Spectrometry. 262, 180–186.

Perrin, C., Prestimonaco, L., Servelle, G., Tilhac, R., Maury, M., Cabrol, P., 2014. Aragonite–calcite speleothems: identifying original and diagenetic features, Journal of Sedimentary Research 84, 245–269.

Pleskot, K., Apolinarska, K., Kolaczek, P., Suchora, M., Fojutowski, M., Joniak, T., Kotrys, B., Kramkowski, M., Slowinski, M., Wozniak, M., Lamentowicza, M., 2020. Searching for the 4.2 ka climate event at Lake Spore, Poland. Catena 191, 104565.

Prasad, S., Enzel, Y., 2006. Holocene paleoclimates of India. Quaternary Research 66, 442–453.

Railsback, L.B., Akers, P.D., Wang, L., Holdridge, G.A., Voarintsoa, N., 2013. Layer-bounding surfaces in stalagmites as keys to better paleoclimatological histories and chronologies. International Journal of Speleology 42, 167–180.

Railsback, L.B., Brook, G.A., Chen, J., Kalin, R., Fleischer, C.J., 1994. Environmental controls on the petrology of a Late Holocene speleothem from Botswana with annual layers of aragonite and calcite. Journal of Sedimentary Research A64, 147–155.

Railsback, L.B., Brook, G.A., Liang, F., Voarintsoa, N.R.G., Cheng, H., Edwards, R.L., 2018a. A multi-proxy climate record from a northwestern Botswana stalagmite suggesting wetness late in the Little Ice Age (1810–1820 CE) and drying thereafter in response to changing migration of the tropical rain belt or ITCZ.   Palaeogeography, Palaeoclimatology, Palaeoecology 506, 139-153.

Railsback, L.B., Liang, F., Brook, G.A., Voarintsoa, N.R.G., Sletten, H.R., Marais, E., Hardt, B., Cheng, H., Edwards, R.L., 2018b. The timing, two-pulsed nature, and variable climatic expression of the 4.2 ka event: a review and new high-resolution stalagmite data from Namibia: Quaternary Science Reviews 186, 78–90.

Railsback, L.B., Kraft, S., Liang, F., Brook, G.A., Marais, E., Cheng, H., Edwards, R.L., 2019. Control of insolation on stalagmite growth, rainfall, and migration of the tropical rain belt in northern Namibia over the last 100 kyr, as suggested by a rare MIS 5b-5c stalagmite from Dante Cave. Palaeogeography, Palaeoclimatology, Palaeoecology 535, 109348.

Ran, M., Chen, L., 2019. The 4.2 ka BP climatic event and its cultural responses. Quaternary International 521, 158-167.

Rashid, H., Polyak, L., Mosley-Thompson, E., 2011 Abrupt climate change revisited, in Rashid, H., Polyak, L., Mosley-Thompson, E., eds., Abrupt Climate Change: Mechanisms, Patterns, and Impacts. Geophysical Monographs Series 193, 1-14.

Schefuß, E., Kuhlmmann, H., Mollenhauer, G., Prange, M., Pätzold, J., 2011. Forcing of wet phases in Southeast Africa over the past 17,000 years. Nature 480, 509–512.

Schlesinger M.E., Ramankutty N., 1994. An oscillation in the global climate system of period 65–70 years. Nature 367:723–726.

Scholz, D., Frisia, S., Borsato, A., Spötl, C., Fohlmeister, J., Mudelsee, M., Miorandi, R., Mangini, A., 2012. Holocene climate variability in north-eastern Italy: potential influence of the NAO and solar activity recorded by speleothem data. Climate of the Past 8, 1367–1383.

Schüller, I., Belz, L., Wilkes, H., Wehrmann, A., 2018. Late Quaternary shift in southern African rainfall zones: sedimentary and geochemical data from Kalahari pans. Zeitschrift für Geomorphologie, 61, 339–362.

Sharifi, A., Pourmand, A., Canuel, E.A., Ferer-Tyler, E., Peterson, L.C., Aichner, B., Feakins, A.J., Daryee, T., Djamali, M., Beni, A.N., Lahijani, H.A.K., Swart, P.K., 2015. Abrupt climate variability since the last deglaciation based on a high-resolution, multi-proxy peat record from NW Iran: The hand that rocked the Cradle of Civilization? Quaternary Science Reviews 123, 215–230.

Shen, C.C., Edwards, R.L., Cheng, H., Dorale, J.A., Thomas, R.B., Moran, S.B., Weinstein, S.E., Edmonds, H.N., 2002. Uranium and thorium isotopic and concentration measurements by magnetic sector inductively coupled plasma mass spectrometry. Chemical Geology 185, 165–178.

Shtober-Zisu, N., Schwarcz, H.P., Chow, T., Omelon, C.R., Southam, G., 2014. Caves in caves: evolution of post-depositional macroholes in stalagmites. International Journal of Speleology 43, 323–334.

Sletten, H.R., Railsback, L.B., Liang, F., Brook, G.A., Marais, E., Hardt, B.F., Cheng, H., Edwards, R.L., 2013. A petrographic and geochemical record of climate change over the last 4600 years from a northern Namibia stalagmite, with evidence of abruptly wetter climate at the beginning of southern Africa's Iron Age. Palaeogeography, Palaeoclimatology, Palaeoecolology 376, 149–162.

Stanley, J.-D., Krom, M.D., Cliff, R.A., Woodward, J.C., 2003. Nile flow failure at the end of the Old Kingdom, Egypt: strontium isotopic and petrologic evidence. Geoarchaeology: An International Journal 18, 395–402.

Staubwasser, M., Sirocko, F., Grootes, P.M., Segl, M., 2003. Climate change at the 4.2 ka BP termination of the Indus valley civilization and Holocene south Asian monsoon variability. Geophysical Research Letters 30, 1425.

Tan, L., Cai, Y., Cheng, H., Edwards, L. R., Gao, Y., Xu, H., Zhang, H., An, Z., 2018. Centennial-to decadal-scale monsoon precipitation variations in the upper Hanjiang River region, China over the past 6650 years, Earth and Planetary Science Letters 482, 580–590.

Thompson, L.G., Mosley-Thompson, E., Davis, M.E., Henderson, K.A., Brecher, H.H., Zagorodnov, V.S., Mashiotta, T.A., Lin, P.-N., Mikhalenko, V.N., Hardy, D.R., Beer, J., 2002. Kilimanjaro ice core records: evidence of Holocene climate change in tropical Africa. Science 298, 589–593.

Tierney, J.E., Oppo, D.W., LeGrande, A.N., Huang, Y., Rosenthal, Y., Linsley, B.K., 2012. The influence of Indian Ocean atmospheric circulation on Warm Pool hydroclimate during the Holocene epoch. Journal of Geophysical Research-Atmospheres 117, D19108.

van Heerden, J., Taljaard, J.J., 1998. Africa and surrounding waters. In: Koroly, D.J., Vincent, D.G. (Eds.), Meteorology of the Southern Hemisphere: Meteorological Monographs of the American Meteorological Society. Vol. 27. pp. 141–174.

van Oldenborgh, G.J., te Raa, L.A., Dijkstra, H.A., Philip, S.Y., 2009. Frequency- or amplitude-dependent effects of the Atlantic meridional overturning on the tropical Pacific Ocean. Ocean Science 5, 293–301.

van Oldenborgh, G.J., Doblas-Reyes, F.J., Wouters, B., Hazeleger, W., Decadal prediction skill in a multi-model ensemble. Climate Dynamics 38, 1263–1280.

Voarintsoa, N.R.G., Brook, G.A., Liang, F., Marais, E., Hardt, B., Cheng, H., Edwards, R.L., Railsback, L.B., 2017a. Stalagmite multi-proxy evidence of wet and dry intervals in northeastern Namibia: linkage to latitudinal shifts of the Inter-Tropical Convergence Zone and changing solar activity from AD 1400 to 1950. The Holocene 27, 384–396.

Voarintsoa, N.R.G., Wang, L., Bruce Railsback, L., Brook, G.A., Liang, F., Cheng, H., Lawrence Edwards, R., 2017b. Multiple proxy analyses of a U/Th-dated stalagmite to reconstruct paleoenvironmental changes in northwestern Madagascar between 370 CE and 1300 CE. Palaeogeography Palaeoclimatology Palaeoecology 469, 138–155.

Vogel, J.C., Fuls, A., Ellis, R.P., 1978. The geographical distribution of kranz grasses in South Africa. South African Journal of Science 74, 209–215.

Wang, L., Brook, G.A., Burney, D.A., Voarintsoa, N.R.G., Liang, F., Cheng, H., Edwards, R.L., 2019. The African Humid Period, rapid climate change events, the timing of human colonization, and megafaunal extinctions in Madagascar during the Holocene: Evidence from a 2m Anjohibe Cave stalagmite. Quaternary Science Reviews 210, 136-153.

Weiss, H., Courty, M.-A., Wetterstrom, W., Guichard, F., Senior, L., Meadow, R., Curnow, A., 1993. The genesis and collapse of third millennium north Mesopotamian civilization. Science 261, 995–1004.

Weiss, H., 2016. Global megadrought, societal collapse and resilience at 4.2-3.9 ka BP across the Mediterranean and west Asia. PAGES 24, 62–63.

Wurtzel, J.B., Abram, N.J., Lewis, S.C., Bajo, P., Hellstrom, J.C., Troitzsch, U., Heslop, D., 2018. Tropical Indo-Pacific hydroclimate response to North Atlantic forcing during the last deglaciation as recorded by a speleothem from Sumatra, Indonesia. Earth and Planetary Science Letters 492, 264–278.

Yadava, M.G., Ramesh, R., Pant, G.B., 2004. Past monsoon rainfall variation in peninsular India recorded in a 331-year-old speleothem. The Holocene 14, 517-524.

Yan, M., Liu, J., 2019, Physical processes of cooling and mega-drought during the 4.2 ka BP event: results from TraCE-21ka simulations. Climate of the Past 277–265 ,15.

Zanchetta, G., Regatierri, E., Isola, I., Drysdale, R.N., Bini, M., Baneschi, I., Hellstrom, J.C., 2016. The so-called "4.2 event" in the central Mediterranean and its climatic teleconnections. Alpine Mediterr. Quat. 29, 5–17.

Zhang, G., Zhu, C., Wang, J., Zhu, G., Ma, C., Zheng, C., Zhao, L., Li, Z., Li, L., Jin, A., 2010. Environmental archaeology on Longshan Culture (4500–4000 aBP) at Yuhuicun Site in Bengbu, Anhui Province. Journal of Geographical Sciences 20, 455-468.

Zhang, H., Cheng, H., Cai, Y., Spötl, C., Kathayat, G., Sinha, A., Edwards, R.L., Tan, L., 2018. Hydroclimatic variations in southeastern China during the 4.2 ka event reflected by stalagmite records. Climate of the Past 1817–1805, 14.

Zhu, X.H., Li, B., Ma, C.M., Zhu, C., Wu,L., Liu, H., 2017. Late Neolithic phytolith and charcoal records of human activities and vegetation change in Shijiahe culture, Tanjialing site, China. PLoS ONE 12(5): e0177287.

Fig. 1. Map of southern Africa showing depictions of the CAB and KD in austral summer by various authors. Red highlights the most recent and detailed of those depictions, as discussed in Section 2.2. Arrows show very generalized wind directions; these winds dictate that humidity is greater on the west or north side of the CAB. The Nicholson (1996) boundary is for January and was reproduced as Fig. 1 in Gasse (2000). The Howard and Washington (2019) CAB and Kalahari Discontinuity are for December, the last month for which they provided a map. The ITCZ is not shown because Nicholson (2018) demonstrated that the ITCZ never comes south of the equator. Gray shading shows the area of January rainfall exceeding 4 mm/day according to the Tropical Rainfall Measuring Mission (TRMM) as shown at https://trmm.gsfc.nasa.gov/trmm_rain/Events/trmm_climatology_3B43.html. Numbers indicate locations of other records discussed in Section 5.3. The underlying base map is from the Alabama Maps website of the Department of Geography of the University of Alabama at

Fig. 2. Images and data from the Type E surface 41.5 mm from the top of Stalagmite DAN1 from Dante Cave in northeastern Namibia. A. Scanned image of the uppermost 10 cm of Stalagmite DAN1. B. Photomicrograph of the Type E surface. The corrosion suggests influx of dilute water and the deposition of detritus suggests influx of much water and possible submergence of the stalagmite. The indexing labels at left are more broadly spaced than one would expect from the scale bar at bottom because the indexing system was generated along the growth axis of the stalagmite, whereas this image is from a location off the growth axis and thus where layers are thinner. C. Age model for uppermost 10 cm of Stalagmite DAN1. D. Plot of C and O stable isotope data along 6 mm of the growth axis of Stalagmite DAN1. The ages and stable-isotope data plotted here are reported in Supplementary Document 1.

Fig. 3. Images and data from the Type E surface 334 mm from the top of Stalagmite DP2 from Dante Cave in northeastern Namibia. A. Scanned image of Stalagmite DP2. B. Photomicrograph of the Type E surface. The corrosion suggests influx of dilute water and the deposition of detritus suggests exceptional influx water. C. Age model for Stalagmite DP2. Three possible inferences for age relationships near the base of the stalagmite are presented. D. Plot of C and O stable isotope data along 9 mm of the growth axis of Stalagmite DP2. The ages and stable-isotope data plotted here are reported in Supplementary Document 1.

Fig. 4. Sketches illustrating that isotopic evidence of rapid climate change to wetter conditions can be removed after deposition. In A, *slow* change to wetter conditions leaves a greater vertical sequence of decreasing $\delta^{18}O$ or $\delta^{13}C$, some but not all of which is removed by corrosion. In B, *fast* change to the same value of $\delta^{18}O$ or $\delta^{13}C$ leaves a smaller vertical sequence of decreasing $\delta^{18}O$ or $\delta^{13}C$, all of which may be removed by the same extent of corrosion. Part B illustrates that failure to recognize surfaces of dissolution (Type E surfaces) may result in failure to recognize rapid climate change to wetter conditions *and* that all isotopic evidence of rapid climate change may be lost to corrosion. The loss of record at such Type E surfaces is analogous to the loss of record at unconformities, the surfaces of erosion, lost strata, and lost history encountered in geology (Hutton, 1788).

[Placement of Fig. 4 near the second paragraph of Section 5.1 would be ideal.]

Fig. 5. Pattern resulting from change from wetter to drier conditions if routine transport of solids by drip water occurs wherein greater drip rate washes solids away and smaller drip rate does not (Yadava et al., 2004). This pattern does not occur in Stalagmites DP2 and DAN1.

Fig. 6. Comparison of timing of evidence of the 4.2 ka Event at Dante Cave in northeastern Namibia (C) and nitrogen-isotope and carbon-isotope evidence of a wet period at Spitzkoppe in west-central Namibia (Chase et al., 2009) (D) with other estimates of the timing of the 4.2 ka Event (A and B). The N and C isotope data were detrended by, for each value of $\delta^{15}N$ or $\delta^{13}C$, subtracting the result of linear regression of the original data over the period from 6000 to 2000 yrs BP. The most negative value of $\delta^{15}N$ and greatest value of $\delta^{13}C$ coincide exactly with evidence of wetness in Stalagmite DP1 and DAN2 and with the age of the event suggested by Case α of the age model for Stalagmite DP2, and more generally with the centroid of ages for the 4.2 ka Event from eleven sites outside Africa.

Fig. 7. Two proxy records of Holocene climate from near Dante Cave. Upward indicates wetter conditions in both panels A. Reconstruction of precipitation during the wettest quarter of the year of Cordova et al. (2017) from pollen and charcoal data at Lake Ngami in northwestern Botswana. Vertical marks show position in time of pollen samples, but vertical positions of those lines have no meaning. B. Carbon isotope composition of sedimentary organic matter at Omongwa Pan in eastern Namibia (Belz et al., 2020). The age data shown in B are from Schüller et al. (2018) available at https://doi.pangaea.de/10.1594/PANGAEA.865040 and not from Table 2 of Belz et al. (2020). Both records are compatible with the wet period at about 4.0 ka inferred from stalagmite data from Dante Cave in northeastern Namibia.

Fig. 8. Map of the Indo-Pacific region showing locations at which proxy evidence of the 4.2 ka Event has been reported (circles and squares) and showing modeling results of Yan and Liu (2019) (underlying shading). Data from Locations 1 to 4 are shown in Figs. 2, 3, 6 and 7 of this paper. Note the general agreement of the proxy data and model results, both of which suggest that the event was not globally dry, and especially not in mid-latitude regions of the Southern Hemisphere, as discussed in Sections 5.3 and 5.4.

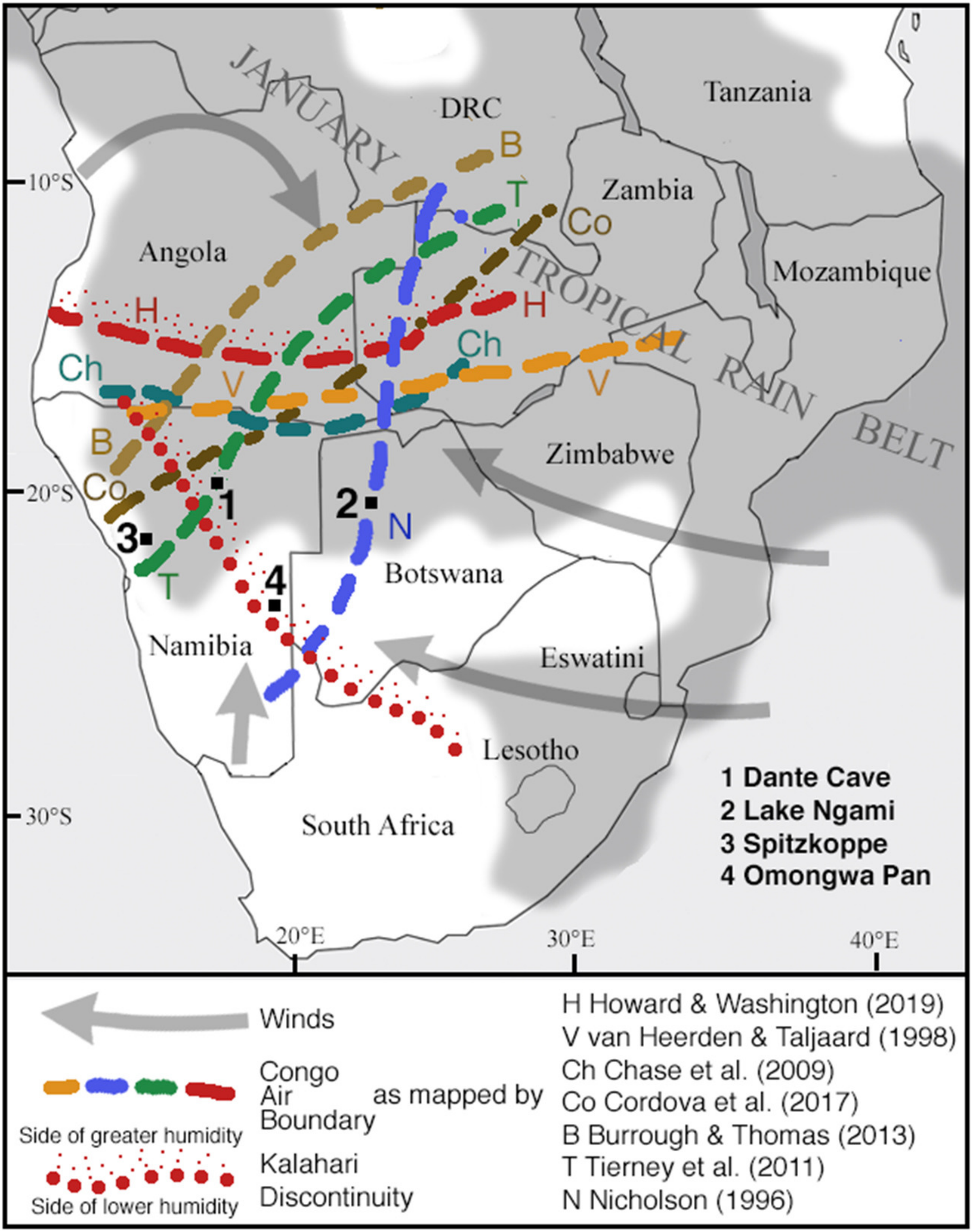

JANUARY
TROPICAL RAIN BELT
DRC
Tanzania
Zambia
Angola
Mozambique
Zimbabwe
Botswana
Namibia
Eswatini
Lesotho
South Africa
10°S
20°S
30°S
20°E
30°E
40°E
B
T
Co
H
Ch
V
N
1
2
3
4
1 Dante Cave
2 Lake Ngami
3 Spitzkoppe
4 Omongwa Pan
Winds
Congo Air Boundary as mapped by
Side of greater humidity
Kalahari Discontinuity
Side of lower humidity
H Howard & Washington (2019)
V van Heerden & Taljaard (1998)
Ch Chase et al. (2009)
Co Cordova et al. (2017)
B Burrough & Thomas (2013)
T Tierney et al. (2011)
N Nicholson (1996)

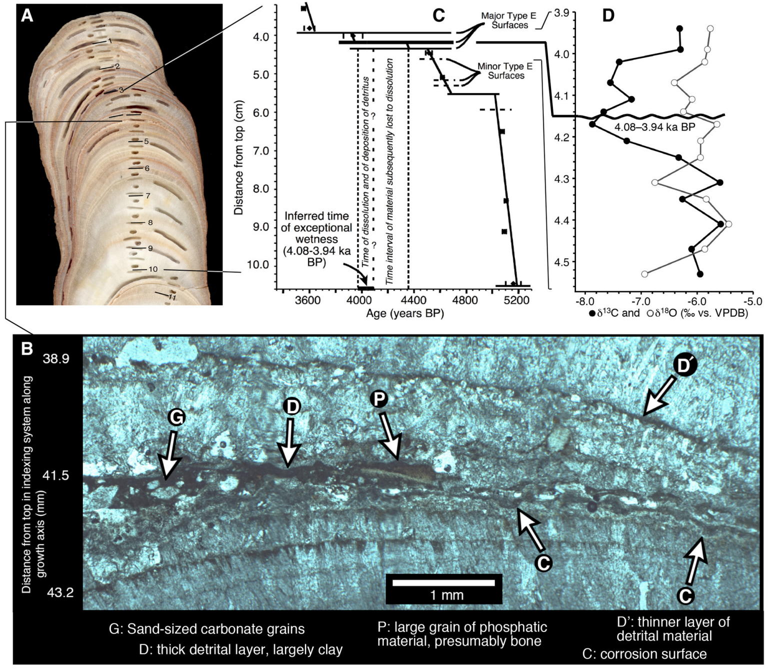

A
1
2
3
5
6
7
8
9
10
11
C
Major Type E Surfaces
Minor Type E Surfaces
Distance from top (cm)
Inferred time of exceptional wetness (4.08-3.94 ka BP)
Time of dissolution and of deposition of detritus
Time interval of material subsequently lost to dissolution
Age (years BP)
D
4.08–3.94 ka BP
δ13C and δ18O (‰ vs. VPDB)
B
38.9
41.5
43.2
Distance from top in indexing system along growth axis (mm)
G
D
P
D′
C
C
1 mm
G: Sand-sized carbonate grains
D: thick detrital layer, largely clay
P: large grain of phosphatic material, presumably bone
D': thinner layer of detrital material
C: corrosion surface

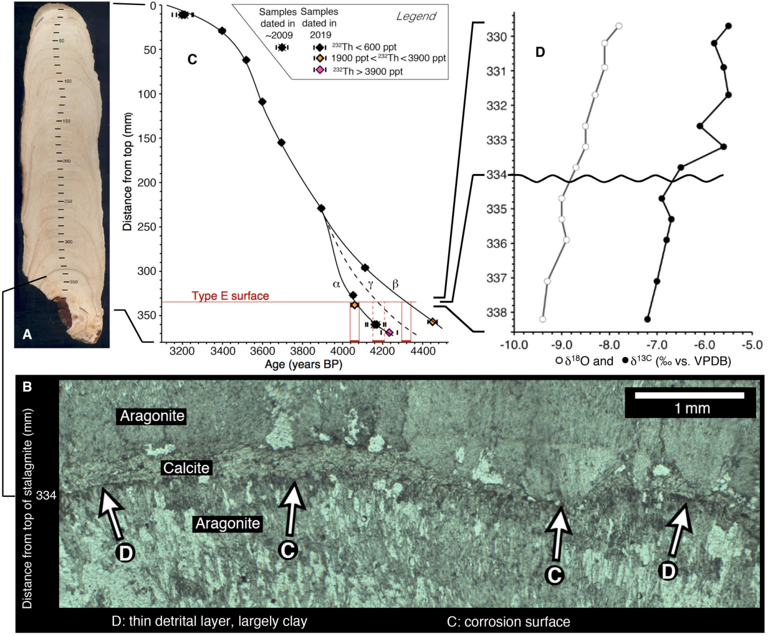

A
C
Samples dated in ~2009
Samples dated in 2019
Legend
$^{232}Th < 600$ ppt
1900 ppt < ^{232}Th < 3900 ppt
$^{232}Th > 3900$ ppt
Distance from top (mm)
Age (years BP)
Type E surface
α
γ
β
D
δ18O and δ13C (‰ vs. VPDB)
B
Aragonite
Calcite
Aragonite
1 mm
Distance from top of stalagmite (mm)
334
D: thin detrital layer, largely clay
C: corrosion surface

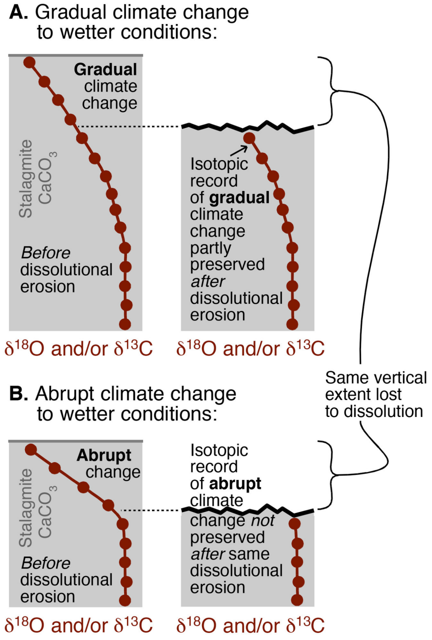
A. Gradual climate change to wetter conditions:
Gradual climate change
Stalagmite $CaCO_3$
Before dissolutional erosion
Isotopic record of gradual climate change partly preserved after dissolutional erosion
$\delta^{18}O$ and/or $\delta^{13}C$
$\delta^{18}O$ and/or $\delta^{13}C$
Same vertical extent lost to dissolution
B. Abrupt climate change to wetter conditions:
Abrupt change
Stalagmite $CaCO_3$
Before dissolutional erosion
Isotopic record of abrupt climate change not preserved after same dissolutional erosion
$\delta^{18}O$ and/or $\delta^{13}C$
$\delta^{18}O$ and/or $\delta^{13}C$

Drier – detritus delivered by drip but not washed from crest

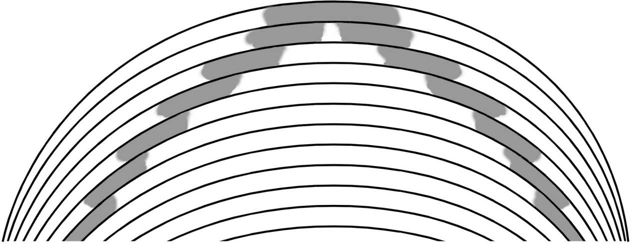

Wetter – detritus delivered by drip but washed from crest by dripwater

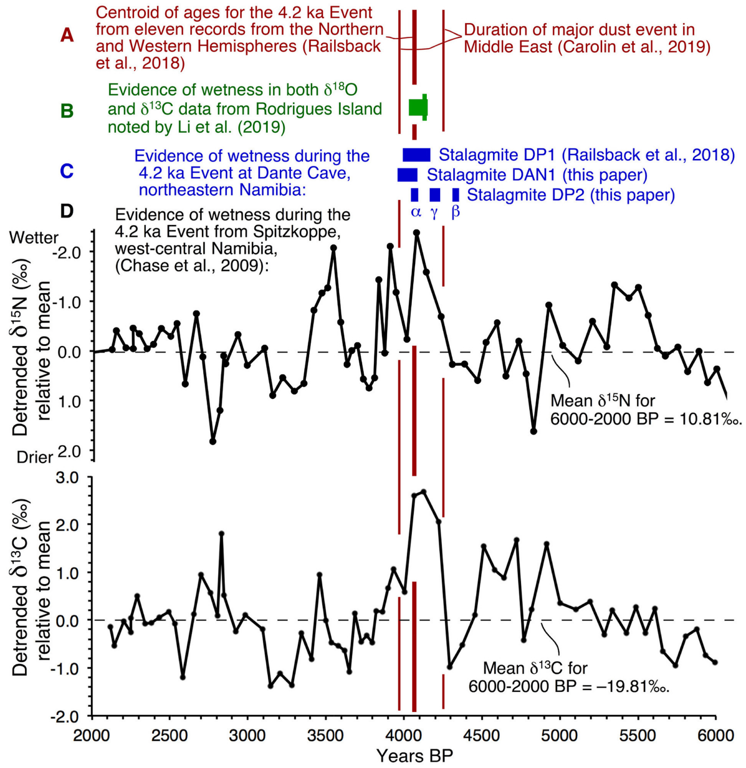
A
Centroid of ages for the 4.2 ka Event from eleven records from the Northern and Western Hemispheres (Railsback et al., 2018)
Duration of major dust event in Middle East (Carolin et al., 2019)
B
Evidence of wetness in both δ18O and δ13C data from Rodrigues Island noted by Li et al. (2019)
C
Evidence of wetness during the 4.2 ka Event at Dante Cave, northeastern Namibia:
Stalagmite DP1 (Railsback et al., 2018)
Stalagmite DAN1 (this paper)
Stalagmite DP2 (this paper)
α γ β
D
Evidence of wetness during the 4.2 ka Event from Spitzkoppe, west-central Namibia, (Chase et al., 2009):
Wetter
Drier
Detrended δ15N (‰) relative to mean
-2.0
-1.0
0.0
1.0
2.0
Mean δ15N for 6000-2000 BP = 10.81‰.
Detrended δ13C (‰) relative to mean
3.0
2.0
1.0
0.0
-1.0
-2.0
Mean δ13C for 6000-2000 BP = –19.81‰.
2000
2500
3000
3500
4000
4500
5000
5500
6000
Years BP

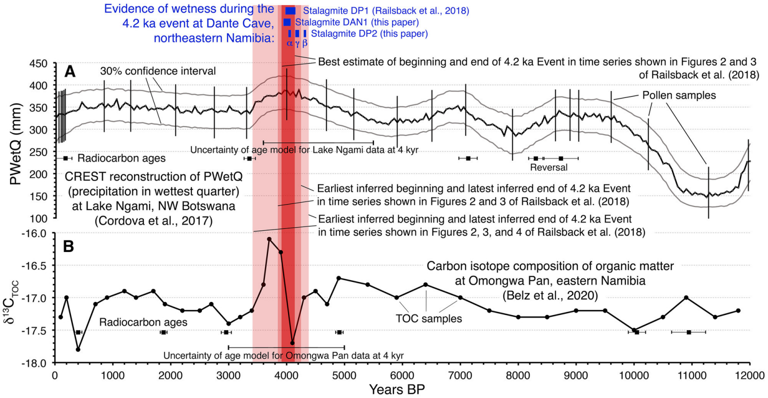

Evidence of wetness during the 4.2 ka event at Dante Cave, northeastern Namibia:
Stalagmite DP1 (Railsback et al., 2018)
Stalagmite DAN1 (this paper)
Stalagmite DP2 (this paper)
α γ β
Best estimate of beginning and end of 4.2 ka Event in time series shown in Figures 2 and 3 of Railsback et al. (2018)
A
30% confidence interval
Pollen samples
PWetQ (mm)
Uncertainty of age model for Lake Ngami data at 4 kyr
Radiocarbon ages
Reversal
CREST reconstruction of PWetQ (precipitation in wettest quarter) at Lake Ngami, NW Botswana (Cordova et al., 2017)
Earliest inferred beginning and latest inferred end of 4.2 ka Event in time series shown in Figures 2 and 3 of Railsback et al. (2018)
Earliest inferred beginning and latest inferred end of 4.2 ka Event in time series shown in Figures 2, 3, and 4 of Railsback et al. (2018)
B
$\delta^{13}C_{TOC}$
Carbon isotope composition of organic matter at Omongwa Pan, eastern Namibia (Belz et al., 2020)
Radiocarbon ages
TOC samples
Uncertainty of age model for Omongwa Pan data at 4 kyr
Years BP

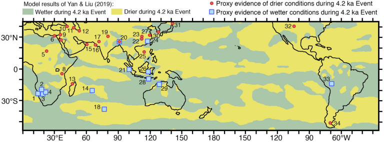

1 Chase et al. (2009) Spitzkoppe inselberg, Namib Desert
2 This article, Dante Cave, Otjozondjupa Region, Namibia
3 Belz et al. (2020) Omongwa Pan, eastern Namibia
4 Cordova et al. (2017) Lake Ngami, northwestern Botswana
5 Kröpelin et al. (2008) Lake Yoa, Ounianga, Chad
6 Stanley et al. (2003) Nile Delta, Gharbia, Egypt
7 Arz et al. (2006) Core GeoB 5836-2, Shaban Deep, Red Sea
8 Thompson et al. (2002) Kilimanjaro ice core, Tanzania
9 Bar-Matthews et al. (1999), Soreq Cave, Jerusalem, Israel
10 Lemcke and Sturm (1997) Lake Van, Turkey
11 Sharifi et al. (2015) Neor Lake, Talesh Mountains, Iran
12 Carolin et al. (2019), Stalagmite GZ14-1, northern Iran
13 Wang et al. (2019) Stalagmite ANJ94-5, Madagascar
14 Li et al. (2018) Rodrigues Island, Indian Ocean*
15 Cullen et al. (2000) Core M5-422, Gulf of Oman
16 Staubwasser et al. (2003) Core 63KA, Indus Delta
Giesche et al., (2019) Core 63KA, Indus Delta
17 Prasad and Enzel (2006) Nal Sarovar Lake, India
18 Li et al. (2020) Amsterdam Island, southern Indian Ocean
19 Nakamura et al. (2016) Lake Rara, Lesser Himalayas
20 Berkelhammer et al. (2012) Stalagmite KM-A, Mawmluh Cave, Meghalaya and Kathayat et al. (2018) Stalagmites ML.1 and ML.2, Meghalaya, India**
21 Wurtzel et al. (2018) Speleothem, Tangga Cave, Indonesia*
22 Zhu et al. (2017) Tanjialing Site, Jianghan Plain, Hubei
23 Liu and Feng (2012) Northern and southern China
24 Zhang et al. (2018) Stalagmite SN17, Shennong Cave, China
25 Dang et al. (2020) Corals, Yongxing Island, South China Sea
26 Tierney et al. (2012) Core BJ8-03-70GGC, Makassar Strait*
27 Zhang et al. (2010) Yuhuicun Site, Bengbu, Anhui
28 Griffiths et al. (2009) Flores Island, Indonesia*
29 Denniston et al. (2013) Stalagmite KN1-51, Australia*
30 Park et al. (2019) Arboreal pollen, southern Korean coast
31 Kawahata (2019) Alkenone-based SSTs, northern Japan
32 Forman et al. (1995) Dunes, northwestern Colorodao, USA***
33 Marchant and Hooghiemstra (2004) Lake Titicaca, Peru/Bolivia***
34 Ohlendorf et al. (2014) Laguna Chaltel, Patagonia

* Map symbols represent inference of Li et al. (2018)
** Map symbols represents inferences of original authors and Li et al. (2018)
*** Map symbols represent inference of Yan and Liu (2019)